

# Chapter 3

---

**Depleted layer of PBTTT-  
C14/MoS<sub>2</sub>-QDs heterojunction for  
enhanced ammonia gas sensitivity**

---

**Abstract**

A highly sensitive, room temperature operating ammonia ( $\text{NH}_3$ ) gas sensor has been fabricated by using PBTTT-C14/ $\text{MoS}_2$ -QDs heterojunction based organic thin film transistor (OTFT). Thin film of PBTTT-C14/ $\text{MoS}_2$ -QDs has been fabricated by low cost and high yield 'floating film transfer method' (FTM). Initially, hydrothermally synthesized  $\text{MoS}_2$  quantum dots (QDs) were added in PBTTT-C14 polymer to make a composite ink, which was used for film fabrication. This polymer/QDs based film has been used as a channel of a top contact-bottom gated organic thin film transistor. Various concentration of  $\text{NH}_3$  ranging from 0.5 to 50 ppm has been exposed on the channel to determine the sensitivity and the selectivity of the device. For comparison, a reference OTFT has been fabricated under the same condition by using pristine PBTTT-C14 thin film. It has been observed that the response of the polymer/QDs heterojunction device is  $\sim 85\%$  at 50 ppm, which is  $\sim 3$  times higher compared to reference device in higher concentration range of  $\text{NH}_3$ . This enhancement becomes possible due to the  $\text{NH}_3$  sensitive depletion layer of polymer/QDs heterojunction. This OTFT sensor shows high selectivity to the  $\text{NH}_3$  gas with good linearity to the concentration, which can fulfill basic requirements for practical utilization.

**3.1. Introduction**

Continuous monitoring of harmful gases produced from different industries and artificial resources becomes a major concern to control environmental pollution, particularly in high population zone [101-103]. Sometimes, human noses are ineffective for many toxic gases if they are odorless or exist in a very low concentration. A reliable gas sensor plays a vital role in monitoring the presence of harmful gases like  $\text{H}_2\text{S}$ ,  $\text{NO}_2$  and volatile organic compounds (VOCs) up to the human olfactory limit and makes the environment acceptable for the human survival [104, 105]. Among the many poisonous and hazardous gases, one of the most harmful and

colorless air contaminants is “ammonia” ( $\text{NH}_3$ ) that has a severe impact on both human beings and the environment [106, 107]. Lower concentration of  $\text{NH}_3$  may cause irritation in the eyes, nose, and throats of humans, and inhaling of an excessive amount of  $\text{NH}_3$  vapors can lead to pulmonary edema [108, 109]. Consequently, it is crucial to monitor the existence of harmful  $\text{NH}_3$  gas in the environment or in different workplaces. Till now, a number of inorganic oxides, different nanostructures and organic semiconductor based  $\text{NH}_3$  gas sensors have been reported. Out of them, metal oxide based  $\text{NH}_3$  sensors are very sensitive and show very good response. However, from the application point of view, their high operating temperature is a big concern. Single nano-crystal like nano-wire, 2D materials based gas sensor show very fast response with high sensitivity, but their fabrication cost, production yield, and tiny active area are the critical bottleneck for commercialization. On the other hand, organic semiconductor based sensor can be fabricated in larger area with high production yield and works at room temperature. Although, their long time stability, selectivity and poor response are the key issues. Therefore, a low-cost, reliable, highly sensitive and room temperature operating  $\text{NH}_3$  gas sensor system is required for commercialization.

To opt the advantageous sides of organic, inorganic nano-structured materials, a numerous organic and inorganic nanostructure hybrids have been investigated up to this point as potential materials for gas detection [27, 110, 111]. Earlier, D. K. Bandgar et al. reported a flexible PANI/ $\alpha\text{-Fe}_2\text{O}_3$  based room temperature operating ammonia sensor with the response of 39% for 100 ppm with low detection limit (LOD) of 5 ppm [112]. Similarly, S. Han et al. have fabricated Poly(3-hexylthiophene)/polystyrene blends based OTFT with 52% response for 50 ppm and 5 ppm LOD [113].

In recent years, transition metal dichalcogenides (TMDs) became a very promising candidate for

chemical gas sensor study due to chemically active sites, room temperature operation, and lower power consumption [114, 115]. Among the TMDs, MoS<sub>2</sub> is a most widely known metal sulfide and is used as a charge donor or acceptor in several sensing applications. Higher specific surface area and strong surface chemistry improves their adsorption between it and the analyte gas, which makes them favorable material with prominent advantages for the gas detection [116, 117]. Quantum Dots (QDs) based materials on the other hand, are highly sensitive for gas sensing applications due to their distinctive properties like higher specific surface area, active edge sites, and quantum confinement effects. Its significant binding interaction with the gas molecules enhances the adsorption capability of the sensor and makes it a potential material for the detection of several kinds of hazardous gases [118, 119]. Instead of a good achievement of those organic/2D hybrid materials based chemical gas sensors, several issues need to be resolved including their faster response, higher stability, and selectivity.

In this study, a hybrid material combination of polythiophene (PTh) based conjugated polymer with TMDs based MoS<sub>2</sub>-QDs has been adopted. PBTTT-C14 [Poly(2,5-bis(3-tetradecylthiophen-2-yl)thieno(3,2-b)thiophene)] attains immense interest from the scientific community due to its superior features like molecular self-ordering,  $\pi$ - $\pi$  stacking, and alkyl side chains. These characteristics of the polymer provide solution processability in commonly available organic solvents and also induce crystallization, which offers significant charge transportation in organic electronic devices [120-122]. Compared to the other conjugated polymers PBTTT-C14 have relatively deep HOMO level resulting higher exhibition of air stability and mobility [123]. Generally, pure conducting polymers possess low sensitivity against the analyte gas. TMDs based MoS<sub>2</sub>-QDs are also promising material for their unique functionality and adaptable surface chemistry. Merging of both the materials makes them suitable for the highly sensitive hybrid

based OTFT ammonia sensor.

Specifically, this study reports a PBTTT-C14/ MoS<sub>2</sub>-QDs heterojunction based OTFT device for the detection of low concentration of ammonia. The chapter firstly described the synthesis of MoS<sub>2</sub>-QDs and fabrication of the pristine polymer and hybrid polymer/QDs based OTFT device *via facile* and cost-effective technique floating film transfer method (FTM). To perform the sensing behavior, OTFT channels are exposed with 0.5 ppm to 50 ppm concentration of the ammonia that shows a very high sensitivity with excellent selectivity.

## **3.2. Experimental Section**

### **3.2.1. Materials**

Sodium molybdate dihydrate (Na<sub>2</sub>MoO<sub>4</sub>·2H<sub>2</sub>O) was obtained from Moly Chem India (purity ≥98%). L-cysteine (HO<sub>2</sub>CCH(NH<sub>2</sub>)- CH<sub>2</sub>SH), Hydrochloric acid, and chloroform (CHCl<sub>3</sub>) were attained from Merck, India. For the preparation of the reagents solution Milli-Q water is used. The organic conjugated polymer poly(2,5-bis(3-tetradecylthiophen-2yl)thieno(3,2-b)thiophene) PBTTT-C14 (Mol. Wt. >40,000) was brought from Sigma-Aldrich Pvt. Ltd. The polymer was used as received without additional purification. Ammonia gas was also purchased from Sigma Aldrich.

### **3.2.2. Synthesis procedure of MoS<sub>2</sub>-QDs**

In this work, the hydrothermal method was chosen for the synthesis of MoS<sub>2</sub>-QDs, since this method is the most commonly used approach for the synthesis of the MoS<sub>2</sub>-QDs and other nano-materials. The focus of this work is to develop an organic/inorganic hybrid p-n heterojunction based highly sensitive ammonia sensor. Therefore, MoS<sub>2</sub> dot was identified to form a better p-n organic/inorganic heterojunction in the composition. From that point of view, the MoS<sub>2</sub>-QDs

have been synthesized *via* a facile and single-step hydrothermal route that can produce ligand free, chemically pure MoS<sub>2</sub> as represented in Fig. 3.1. For this, sodium molybdate dihydrate and L-cysteine (1:2 w/w) dissolved separately in 25 ml of Milli-Q water under constant stirring for 15 min. Afterward, both solutions were slowly mixed together under continuous stirring at a maintained temperature of 40°C to make a homogeneous solution. During this mixing, pH is maintained at ~3 with concentrated HCl.

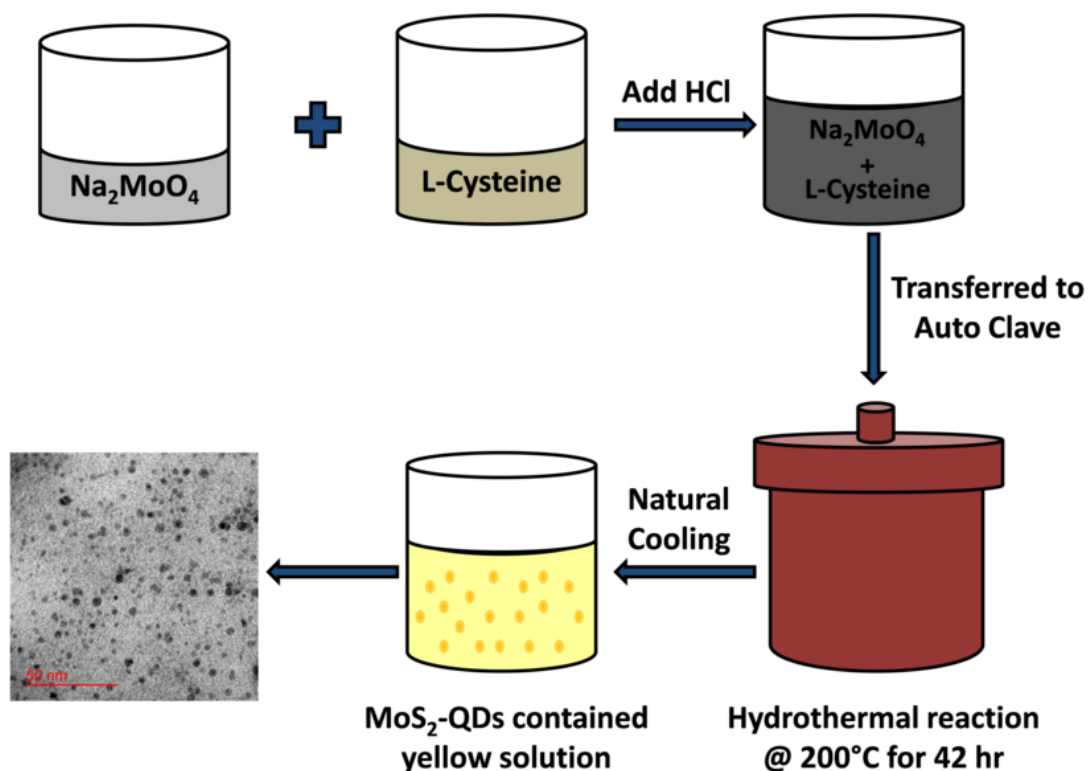


**Fig. 3.1.** Schematic demonstration of hydrothermal synthesis of MoS<sub>2</sub>-QDs.

Subsequently, for the hydrothermal synthesis, this homogeneous solution is then transferred into a Teflon autoclave (100 ml capacity) lined with stainless steel and left for 42 hr at ~ 200°C in the oven. After completion of the process, the oven was allowed to cool down naturally at room temperature. Finally, a light yellowish colloidal solution of MoS<sub>2</sub>-QDs was obtained. For the

purification process, the solution was dialyzed for about 3-4 days in a dialysis bag (Molecular Weight = 2000 Da).

### **3.2.3. Synthesis of PBTTT-C14/ MoS<sub>2</sub>-QDs nanocomposite thin film**

Prior to the synthesis of PBTTT-C14/MoS<sub>2</sub>-QDs hybrid nanocomposite, the phase transfer method has been used to carry MoS<sub>2</sub>-QDs from water to chloroform for the composite preparation, as shown in Fig. 3.2(a). The hydrothermally synthesized homogeneous aqueous solution of MoS<sub>2</sub>-QDs is sonicated rigorously and then added with an equal amount of chloroform (CHCl<sub>3</sub>). In this bi-phase immiscible solution of water and CHCl<sub>3</sub>, the heavier CHCl<sub>3</sub> remains at the bottom and the aqueous dispersion remain at the top. To transfer QDs into chloroform, the immiscible solution is sonicated for 2-3 hr. After completing the sonication process, the aqueous solution has been taken out from the top and remained part is the transferred QDs in chloroform.

For the composite preparation, as shown in Fig. 3.2(a) 10 µl of the extracted solution of QDs/CHCl<sub>3</sub> was mixed in the anhydrous chloroform solution of 2 mg polymer with 10 mg ml<sup>-1</sup> concentration. The composite solution is sonicated for the well dispersion of QDs in polymer. For the composite film casting, low cost and high yield floating film transfer method (FTM) has been used [124]. In this method, a small amount (~10 µl) of polymer/QDs blend was dropped at the center of a petri-dish with diameter of 15 cm, containing hydrophilic liquid substrate (ethylene glycol and glycerol with ratio of 3:1) in ambient conditions as shown in Fig. 3.2(b). As prepared film over the liquid substrate will be transferred to the desired cleaned Si/SiO<sub>2</sub> substrate and dried at 80°C under the flow of nitrogen for the fabrication of the OTFT.

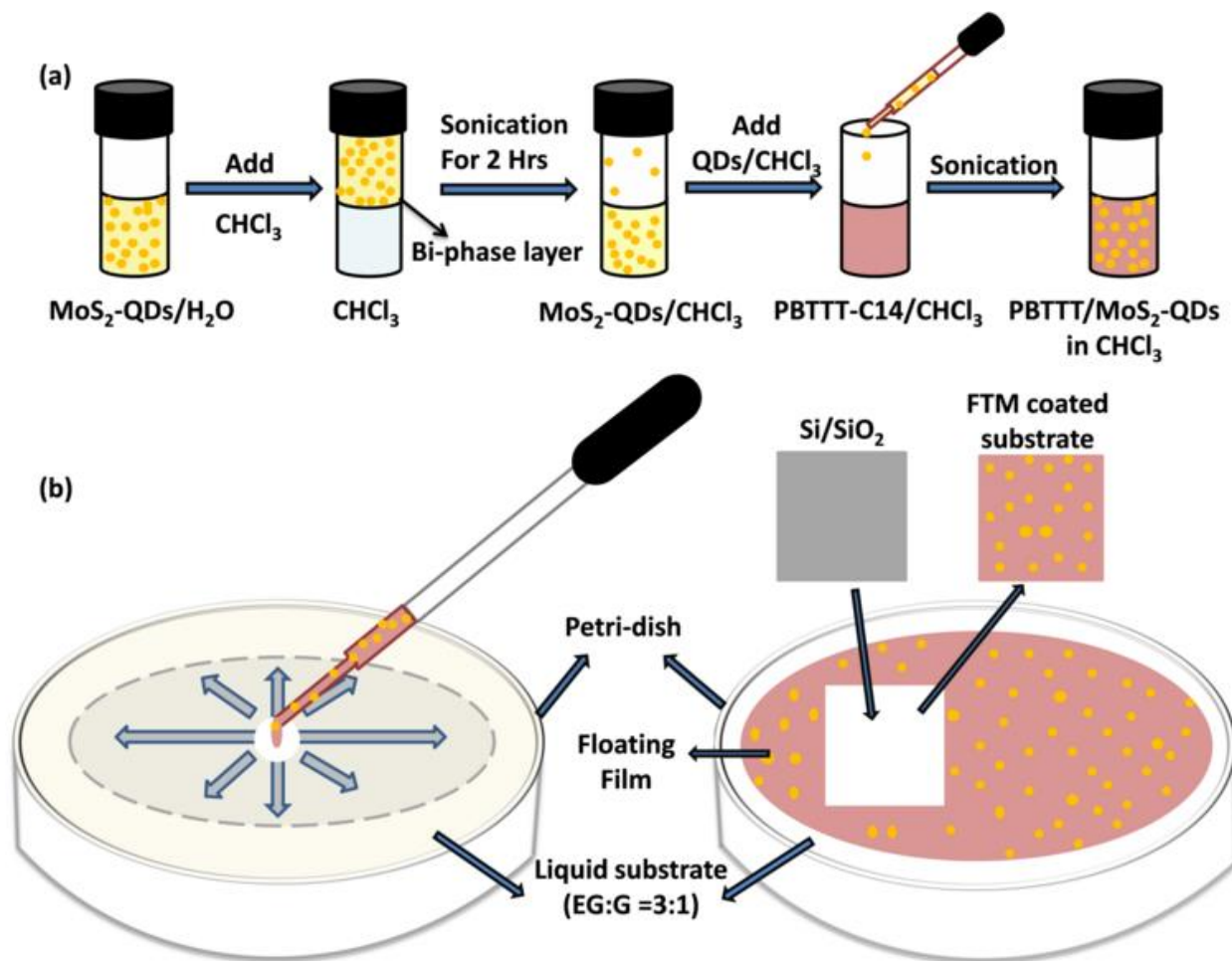


**Fig. 3.2.** Schematic illustration of (a) Phase transfer method to transfer MoS<sub>2</sub>-QDs from water to chloroform; (b) FTM method for PBTTT-C14/MoS<sub>2</sub>-QDs based hybrid film spreading on the nonvolatile liquid substrate (EG:G = 3:1) and stamping of the film on the substrate.

During this process, we have optimized the polymer/QDs solution for the film quality and the sensing performance of the device. Throughout this optimization, in our observation, higher ratio of MoS<sub>2</sub> leads to the breakage in the film that provides a poor device performance. Again, low concentration of MoS<sub>2</sub> reduces the sensitivity of the OTFT due to reduced depleted area of the film. The optimized ratio composite film over the liquid surface was transferred onto a carbon coated grid for the TEM study.

**3.2.4. Device fabrication**

For the bottom gate-top contact OTFT device fabrication, heavily p-doped silicon ( $p^+$ -Si) substrates are used with 300 nm thermally grown  $\text{SiO}_2$  as the gate dielectric. Those  $p^+$ -Si/ $\text{SiO}_2$  substrates are first properly cleaned using four different solvents, including soap solution, deionized water, acetone and isopropanol in an ultrasonic cleaner and dried at  $80^\circ\text{C}$  under the flow of nitrogen. After the cleaning process, the polymer/QDs layer (sensing layer) was transferred over the cleaned Si/ $\text{SiO}_2$  substrate *via* pre described FTM technique. The formation of source-drain electrodes was subsequently deposited on the top of semiconducting film coated substrate by thermal vacuum evaporation of Au through an interdigitated shadow mask with the evaporation rate of  $1.5 \text{ \AA/s}$  at vacuum  $6 \times 10^{-5}$  Torr. The length (L) and width (W) of the interdigitated channel were  $50 \mu\text{m}$  and  $18 \text{ mm}$ , respectively.

**3.2.5. Characterization**

The TEM micrographs with selected area electron diffraction (SAED) patterns were obtained via TECHNAI G<sup>2</sup>20 TWIN (New Zealand) over Cu grid. To achieve the absorption spectra of hydrothermally synthesized  $\text{MoS}_2$ -QDs, quartz cuvette (1 cm optical path length) was used in UV–Vis Epoch 2 micro-plate reader Biotech (USA) spectrophotometer. FT-IR analysis of QDs was done by Thermo Scientific Nicolet 6700 FTIR spectrometer (Germany). Lastly, the electrical (current-voltage) characteristics of the fabricated OTFTs were performed by a semiconductor device analyzer (Keysight B1500A). We have used a gas sensing chamber for the ammonia sensing measurement of the fabricated OTFT, as illustrated in the previous study [125].

### 3.3. Results and discussion

#### 3.3.1. Characterizations of MoS<sub>2</sub>-QDs and nanocomposite thin film

The MoS<sub>2</sub>-QDs were synthesized through facial and single-step hydrothermal route by employing sodium molybdate and L-cysteine as the sources of molybdenum and sulfur, respectively. Synthesized water soluble QDs were characterized by TEM, SAED pattern, FT-IR, and UV-Vis spectroscopy. Fig. 3.3(a) and 3.3(b) represents the TEM images of the synthesized MoS<sub>2</sub>-QDs, which indicates that the QDs are well dispersed in water and distributed homogeneously on copper grid. The average diameter of the synthesized QDs is  $3.3 \pm 0.86$  nm as shown in the size distribution histogram (Inset, Fig. 3.3(a)). The SAED pattern at the inset of Fig. 3.3(b) suggests the crystalline nature of the QDs. Fig. 3.3(c) represents the FT-IR spectra of synthesized QDs, which exhibit a broad and strong peak at 3150-3500 cm<sup>-1</sup> attributed to the -NH<sub>2</sub> and -OH stretching. A major frequency peak at 1633 cm<sup>-1</sup> corresponds to the -C=O stretching vibration due to the presence of the -COOH group. The Smaller peaks at 1056 cm<sup>-1</sup> and 1413 cm<sup>-1</sup> were assigned to the -CN and -NH stretching vibrations of aromatic and aliphatic amines. Fig. 3.3(d) represents the UV-Vis spectra with the absorption peak at 272 nm of dialyzed MoS<sub>2</sub>-QDs, which may be attributed to the excitonic feature of the MoS<sub>2</sub>-QDs and also presents the surface absorbed functional group -NH<sub>2</sub>, which can be confirmed from the FT-IR spectra [126]. The calculated band gap of MoS<sub>2</sub> is 4.2 eV, which is obtained from Tauc's plot (Inset, Fig. 3.3(d)). This value is higher than 2D single-layer MoS<sub>2</sub> (1.9 eV) and bulk MoS<sub>2</sub> (1.2 eV). The increment in the direct band gap energy with respect to the bulk and 2D monolayer MoS<sub>2</sub> is due to the strong quantum confinement effect that led to the enhanced band gap opening.

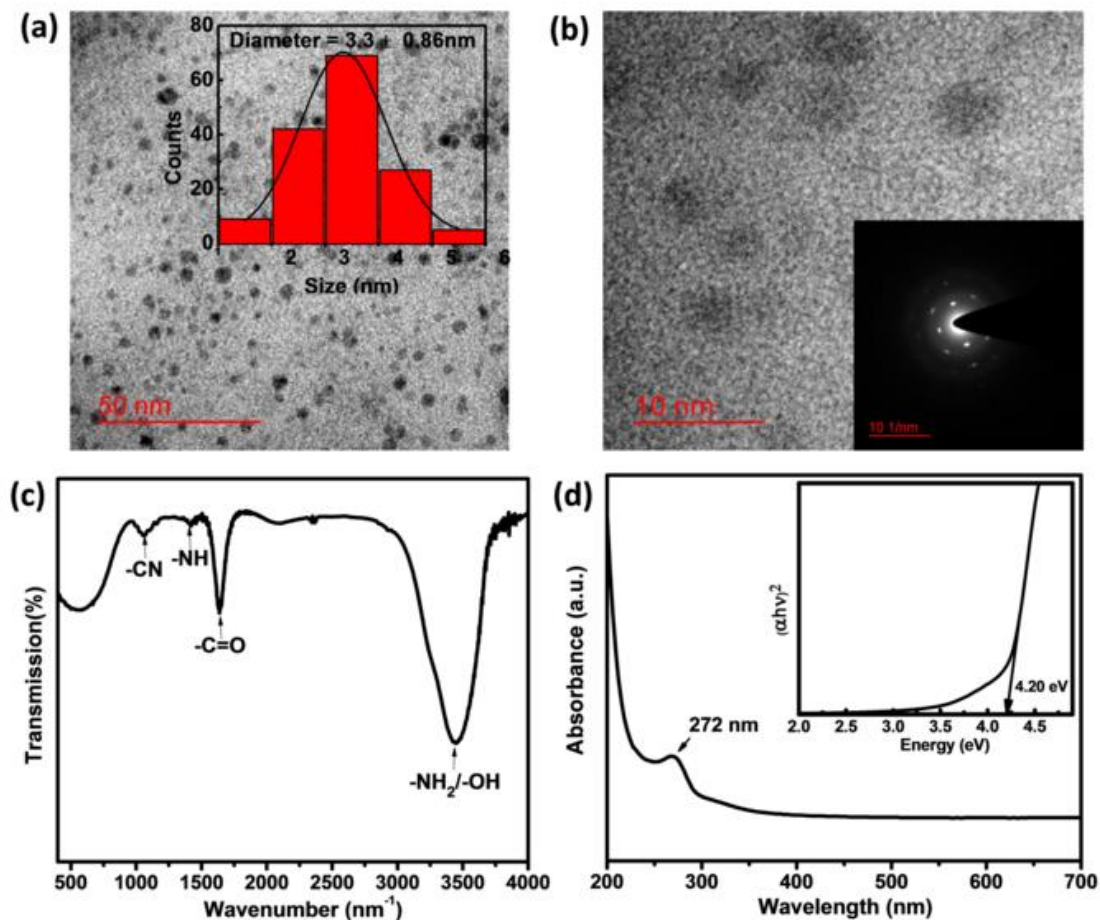


**Fig. 3.3.** (a) TEM image of synthesized MoS<sub>2</sub>-QDs and size distribution histogram, (inset); (b) HR-TEM image and SAED pattern (inset); (c) FT-IR, and; (d) UV-Vis spectra and band gap (inset) of MoS<sub>2</sub>-QDs.

For the PBTTT-C14/MoS<sub>2</sub>-QDs hybrid nanocomposite based thin film characterization, TEM micrographs are shown in Fig. 3.4. The hybrid film has been lifted over the copper grid *via* predefined FTM method. As shown in Fig. 3.4(a), and 3.4(b), low and high resolution TEM images indicate that the QDs are homogeneously distributed on the polymer film. Fig. 3.4(c) represents the SAED pattern of the same, which is in the form of hazy ring pattern. This hazy ring pattern is due to the presence of excessive amount of polymer compared to the MoS<sub>2</sub>-QDs.

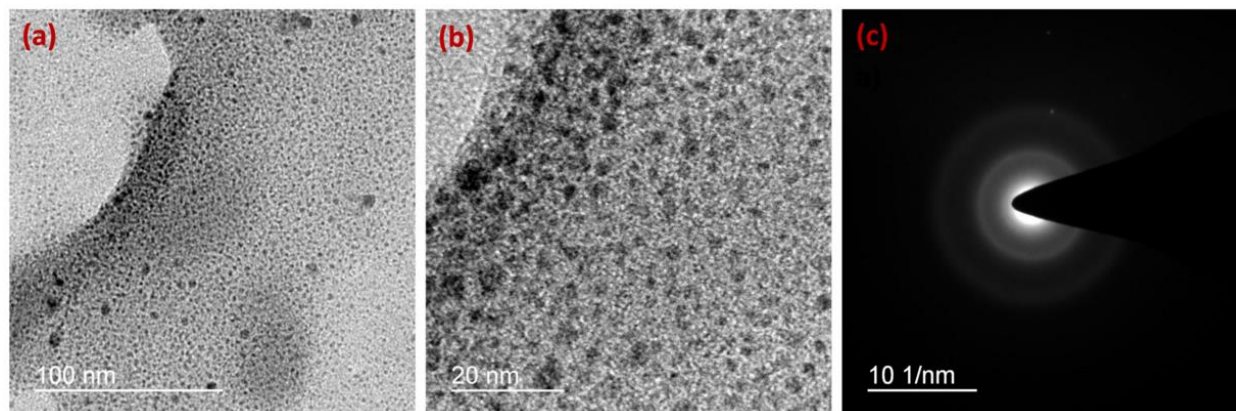


**Fig. 3.4.** TEM image (a) Low resolution, (b) High resolution; and (c) SAED pattern of PBTTT-C14/MoS<sub>2</sub>-QDs FTM film casted over Cu grid.

### 3.3.2. Electrical Characterizations

Schematic of the assemblies, output ( $I_{DS}$ - $V_{DS}$ ) and transfer ( $I_{DS}$ - $V_{GS}$ ) characteristics of the fabricated pristine PBTTT-C14 (Device-1) and PBTTT-C14/MoS<sub>2</sub>-QDs (Device-2) hybrid film based devices are shown in Fig. 3.5. The output characteristics ( $I_{DS}$ - $V_{DS}$ ) of the fabricated devices have been measured at 25°C (room temperature with 50% RH) under dark and plotted over the swept drain voltage range from 0 to -30 V with different constant bias gate voltages as represented in Fig. 3.5(c) and 3.5 (d). And it is found that at the fixed gate bias voltage, drain current is much higher in the polymer/QDs film based OTFT compared to the pristine polymer film. The improvement in the drain current is may be due to the intercalation of the MoS<sub>2</sub>-QDs in the polymer matrix, which facilitates the charge transportation in the semiconducting (sensing) layer of the hybrid based OTFT. Moreover, presence of MoS<sub>2</sub> -QDs in polymer matrix also enhances the ammonia sensing capability of the hybrid film based transistor, which is discussed in the later section.

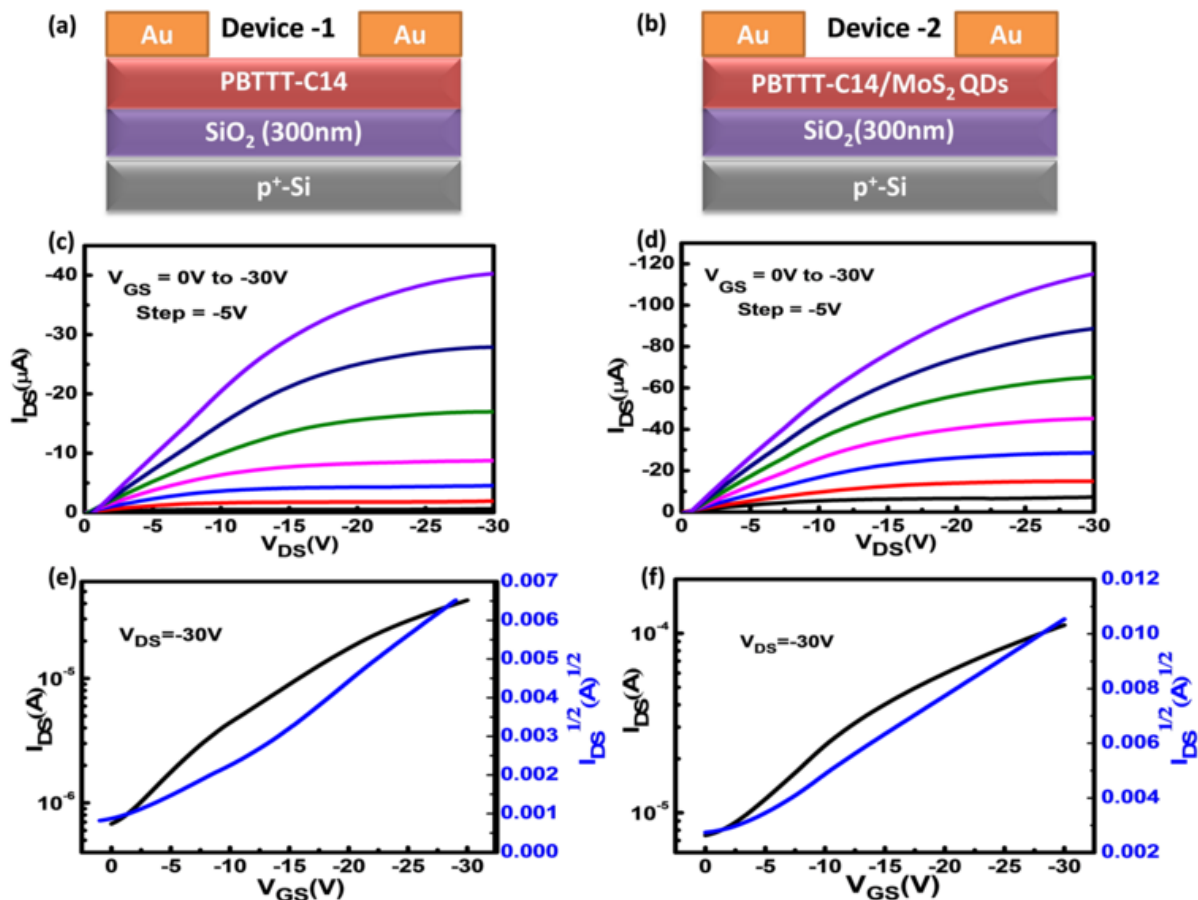


**Fig. 3.5.** Schematic representation of (a) pristine PBTTT-C14 OTFT (Device-1) (b) PBTTT-C14/MoS<sub>2</sub>-QDs OTFT (Device-2); Output characteristics ( $I_{DS}$ - $V_{DS}$ ) of as fabricated (c) Device-1 (d) Device-2; Transfer characteristics ( $I_{DS}$ - $V_{GS}$ ) of as fabricated (e) Device-1 (f) Device-2.

The transfer ( $I_{DS}$ - $V_{GS}$ ) characteristics of the fabricated OTFTs measured at constant drain voltage of -30 V over the swept gate voltage range from 0 to -30 V represented in Fig. 3.5(e) and 3.5(f). Transfer characteristics of OTFTs can be used to extract the important electrical parameters of the transistor as threshold voltage ( $V_{TH}$ ) and mobility ( $\mu$ ). The key parameters of OTFTs can be calculated from the following equation [27]:

$$\sqrt{I_{DS}} = \sqrt{\frac{W\mu C}{2L}} (V_{GS} - V_{TH}) \quad (3.1)$$

Where  $I_{DS}$  represents the saturation drain current under pinch-off condition,  $L$  and  $W$  are symbolized as the length and width of the fabricated OTFT channel, respectively, and  $C$  is the capacitance per unit area of the oxide dielectric layer which was  $10 \text{ nFcm}^{-2}$ . The threshold voltage of the as fabricated OTFT can be calculated by extrapolation of the line corresponding to  $I_{DS}^{1/2}$  versus  $V_{GS}$  curve at  $V_{DS} = -30 \text{ V}$ .

### 3.3.3. Ammonia Sensing

The ammonia sensing experiment of the fabricated OTFTs has been performed inside a chamber as illustrated in the previous study [125]. Under the controlled flow of dry air mixed with analyte  $\text{NH}_3$  gas, both pristine PBTTT-C14 and PBTTT-C14/ $\text{MoS}_2$ -QDs hybrid film based OTFT device channels are exposed with ammonia ranging from 0.5 ppm to 50 ppm at  $25^\circ\text{C}$  (room temperature) under  $\sim 50\%$  relative humidity (RH) condition. For the sensing analysis, transfer characteristics ( $I_{DS}$ - $V_{GS}$ ) of the fabricated OTFTs are measured with various concentrations of ammonia. During this measurement, the gate voltage of the device swept in the range of 0 to -30 V with a fixed drain bias of -30 V. The transfer characteristics of Device-1 and 2 under different concentrations of  $\text{NH}_3$  have been represented in Fig. 3.6(a) and 3.6(b) respectively. From the transfer characteristics it is observed that the drain current ( $I_{DS}$ ) decreases as the concentration of the ammonia increases. The decrease in drain current is attributed to the chemical interaction between ammonia and the exposed active sensing material in the OTFT device channels, which is discussed later in the sensing mechanism section. The decrement in the drain current ( $\Delta I_D$ ) under fixed gate voltage can be calculated by taking the difference between the drain current before and after exposure of the gas. This  $\Delta I_D$  also represents the response of the OTFTs due to

the exposure of the gas which is discussed in the following section. As shown in Fig. 3.6, the reduction in the drain current ( $\Delta I_D$ ) in the transfer characteristics ( $I_{DS}$ - $V_{GS}$ ) of Pristine PBTTT-C14 based OTFT is significantly lower as compared to the hybrid based PBTTT-C14/ MoS<sub>2</sub>-QDs based OTFT. This result reveals the NH<sub>3</sub> sensitivity of this PBTTT-C14 OTFT can be enhanced notably by adding MoS<sub>2</sub>-QDs.

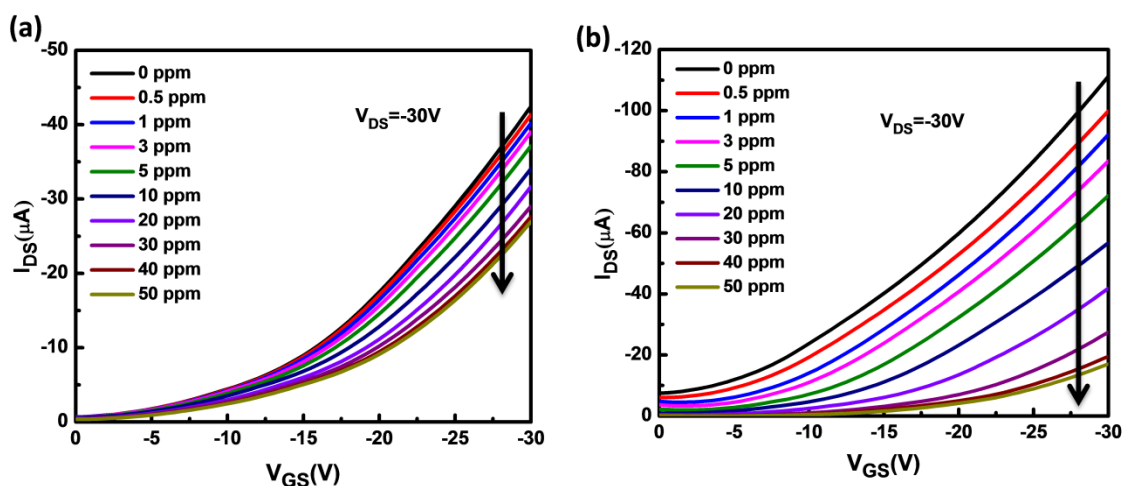


**Fig. 3.6.** Transfer characteristics ( $I_{DS}$ - $V_{GS}$ ) of as fabricated OTFT ammonia sensor at  $V_{DS} = -30V$  with various concentrations (0.5 ppm-50 ppm) (a) pristine PBTTT-C14 and (b) PBTTT-C14/MoS<sub>2</sub>-QDs hybrid film based OTFT.

It is also noted that, in addition to the decrement in drain current ( $\Delta I_D$ ), various electrical parameters of OTFT, such as threshold voltage ( $V_{TH}$ ), and effective carrier mobility ( $\mu_h$ ) changes due to the exposure of NH<sub>3</sub> gas. The variation in physical parameters of the PBTTT-C14/MoS<sub>2</sub>-QDs based OTFT after the exposure of ammonia is given in the below Table-3.1.

Table-3.1: Variation of device parameters and the response of PBTTT-C14 (Device-1) vs. PBTTT-C14/MoS<sub>2</sub>-QDs (Device-2) based OTFT sensors with different concentrations of NH<sub>3</sub>.

NH <sub>3</sub> (ppm)	On current I <sub>on</sub> (μA)		Effective Mobility μ <sub>h</sub> (cm <sup>2</sup> V <sup>-1</sup> sec <sup>-1</sup> )		Threshold voltage V <sub>TH</sub> (V)		Change in Threshold voltage (ΔV <sub>TH</sub> )	Response (%)	
	Device -1	Device- 2	Device -1	Device- 2	Device -1	Device -2		Device -1	Device -2
0	42.48	-111.15	0.0302	0.0450	-2.5	7.56	0	0	0
0.5	41.35	-99.93	0.03	0.0441	-2.59	5.08	2.48	2.66	10.14
1	40.21	-92.08	0.0294	0.0438	-2.77	3.49	4.07	5.35	17.15
3	39.04	-83.31	0.0291	0.0430	-3.22	1.54	6.02	8.09	24.91
5	37.16	-72.23	0.0287	0.0426	-3.6	-1.13	8.69	12.52	35.08
10	34.08	-56.54	0.028	0.0414	-4.19	-3.22	10.78	19.76	48.99
20	31.68	-41.77	0.0268	0.0395	-4.48	-6.56	14.12	25.42	62.38
30	29.02	-27.46	0.0261	0.0346	-4.92	-10.59	18.15	31.69	75.30
40	27.60	-19.61	0.0245	0.0305	-5.18	-11.27	18.83	35.02	82.43
50	26.95	-17.30	0.024	0.0279	-5.72	-11.53	19.09	36.57	84.66

From the Table-3.1, it is clearly noticeable that the shift in the threshold voltage is huge as the increase in ammonia concentration, which is a good signature for the gas sensing application. Besides, the effective carrier mobility of the QDs based hybrid device also gradually decreases with the increasing concentration of ammonia.

### 3.3.4. Gas response and limit of detection

Fig. 3.7 illustrates the dynamic sensing response of the pristine PBTTT-C14 and PBTTT-C14/MoS<sub>2</sub>-QDs hybrid film based OTFT sensor against various NH<sub>3</sub> concentrations ranging from 0.5 to 50 ppm. Ammonia gas is exposed on the fabricated OTFT channels and the response (R) of the sensor can be calculated by using equation [127]:

$$R = \frac{|I_{DS,Air} - I_{DS,Gas}|}{|I_{DS,Air}|} \times 100\% \quad (3.2)$$

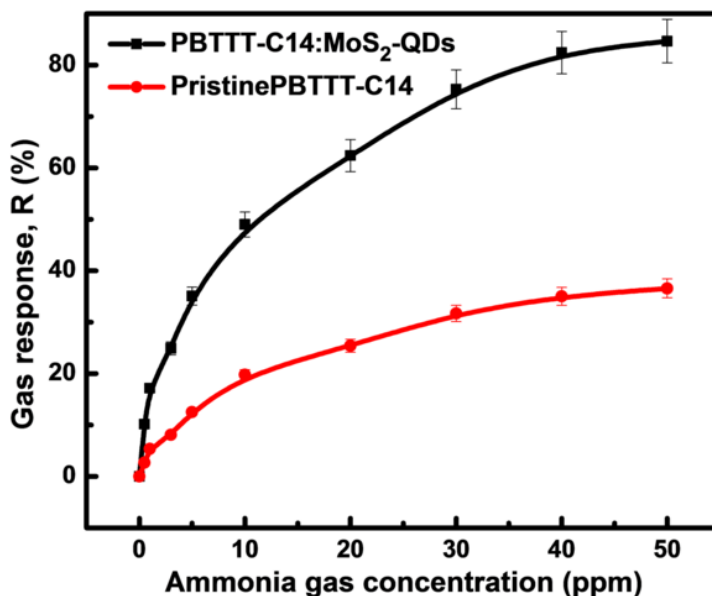


**Fig. 3.7.** Gas response graph of pristine PBTTT-C14 and PBTTT-C14/MoS<sub>2</sub>-QDs hybrid based OTFTs for different NH<sub>3</sub> gas concentration ( $V_{DS} = -30$  V and  $V_{GS} = -30$  V).

The response graph of Device-1 and 2 presented in Fig. 3.7 suggests that the incorporation of QDs in polymer matrix created a remarkable improvement in the response data, particularly in the high concentration range of NH<sub>3</sub>. At 50 ppm concentration of NH<sub>3</sub>, the pristine polymer based OTFT sensor response (sensitivity) is 36.5%, while the polymer/QDs composite based OTFT sensor exhibits 84.66%. In addition, polymer/QDs based sensor shows quite good response even at lower concentration of ammonia.

The another important parameter of the fabricated sensor, called limit of detection (LOD), can be calculated by the following equation [128]:

$$\text{Limit of detection (LOD)} = \frac{3 * \sigma_{rms}}{m} \quad (3.3)$$

Where  $\sigma_{rms}$  represents the root-mean-square deviation of the linear fitting of the curve and the baseline, and 'm' symbolizes the plotted curve's slope. The extracted value of LOD for the fabricated polymer/QDs based sensor has been found to be 0.317 ppm, which is extremely small and indicates its applicability up to a very low concentration limit of NH<sub>3</sub>.

Besides, we perform the transient response of the OTFT for different concentrations of NH<sub>3</sub>, which is given in Fig. 3.8. It has been observed that the variation of the drain current increases with analyte gas, but the rise time remains almost the same for all concentrations (~2 sec.). Besides, the sensor has good linearity in the response at lower concentrations of NH<sub>3</sub>. But at higher concentration, after removing analyte gas, the decay time increases with NH<sub>3</sub> gas concentration. Most likely, it is due to the chemisorption of the NH<sub>3</sub> gas molecule with the semiconducting layer that takes longer time to recover.

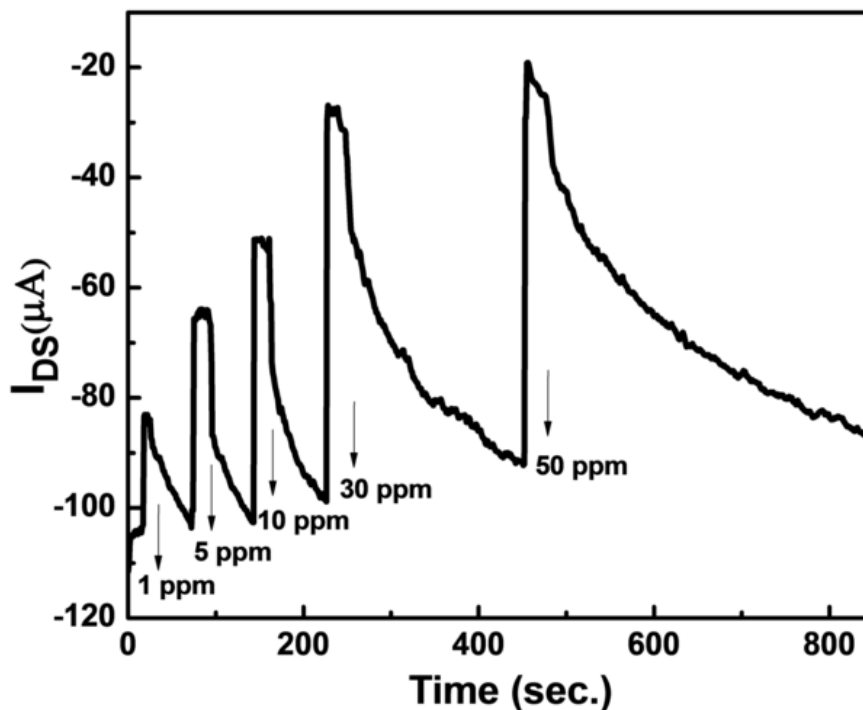


Fig. 3.8. Transient response curve ( $I_{DS}$ -t) of the OTFT sensor for various concentrations of  $NH_3$ .

### 3.3.5. Selectivity

Selectivity can be defined as the ability of the sensor to respond to the specific gas in the existence of other commonly present interfering gases. The fabricated polymer/QDs film based OTFT sensor has negligible gas response towards 50 ppm of other oxidative, reductive and commonly available environmental interfering gases such as methane ( $CH_4$ ), propane ( $C_3H_8$ ), carbon dioxide ( $CO_2$ ), carbon monoxide ( $CO$ ) as shown in Fig. 3.9. For this measurement, the device channel has been exposed with individual interfering gas mixed with the controlled flow of dry air. Higher  $NH_3$  response of the polymer/QDs film based sensor comparative to other interfering gases can be attributed to the high electron donating capability of the  $NH_3$  gas. It is clearly

visible from the selectivity graph that the composite based sensor is highly selective for the low concentration of the ammonia.

For the selectivity analysis of the sensor, we have also investigated the effect of  $\text{NO}_2$  gas. As  $\text{NO}_2$  is a strong oxidizing gas, it will lead to a huge change in  $I_{\text{DS}}$  of the fabricated device in the negative direction to the  $\text{NH}_3$  gas (reducing gas). We have examined the selectivity of the other gases at 50 ppm, similarly we have done this for the same concentration of  $\text{NO}_2$  for the fabricated device. But in the presence of 50 ppm of this strongly oxidizing gas, the device gets damaged. Damaging of the device may be due to its highly oxidizing electron affinity effect, which is one limitation of this device.

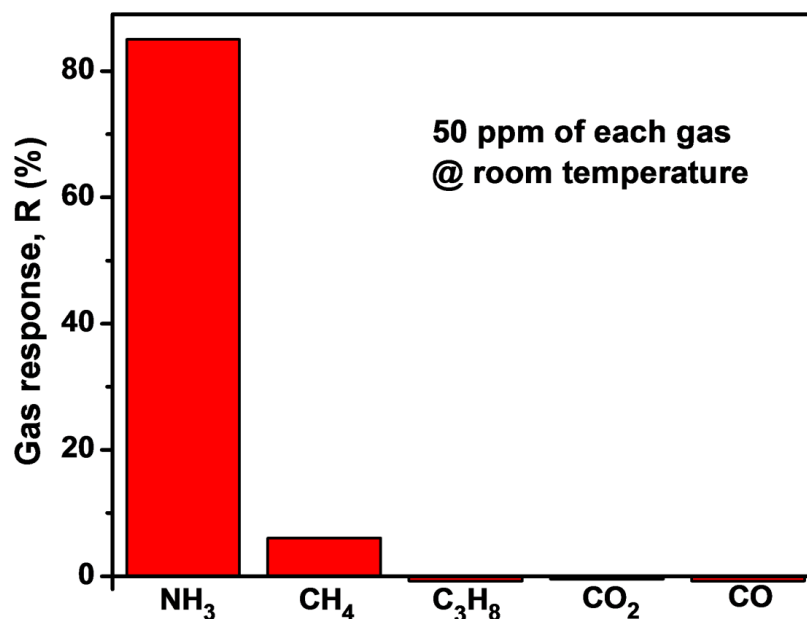


**Fig. 3.9** Selectivity graph of PBTTT-C14/MoS<sub>2</sub>-QDs hybrid based sensor over common interfering gases.

### 3.3.6. Reliability analysis

For the reliability test of the polymer/QDs film based OTFT ammonia sensor, the effect of RH on  $I_{DS}$  (with and without gas) has been investigated, and it has been observed that the response of the sensor is reduces by 8% when RH has been changes from 20% to 80% humidity range for 50 ppm concentration of ammonia as shown in Fig. 3.10, which is negligibly low variation w.r.t the overall  $NH_3$  gas response of the device.

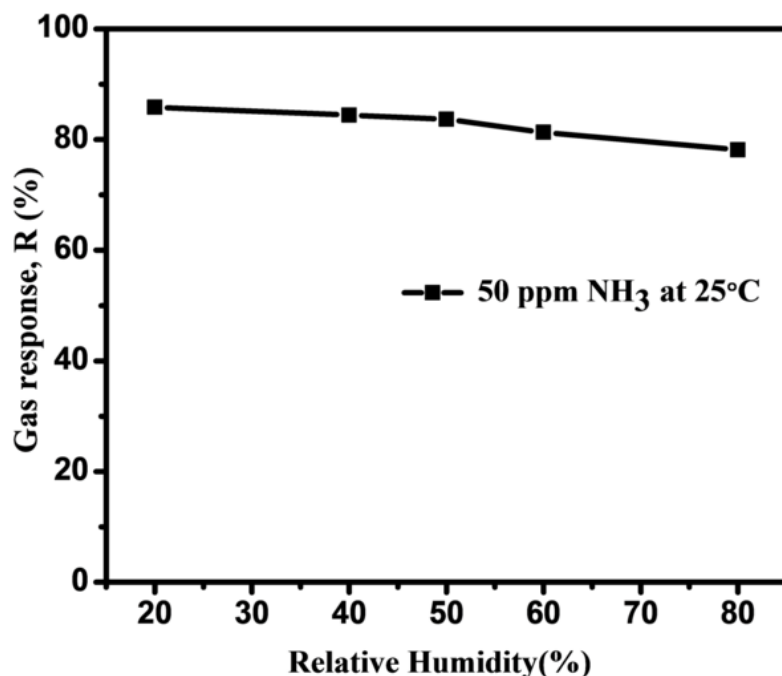


**Fig. 3.10.** Gas response of the PBTTT-C14/MoS<sub>2</sub>-QDs hybrid based OTFT sensor with the variation of relative humidity.

Besides, we have examined two different types of stabilities. First one is the environmental stability, which has been tested for 25 consecutive days. During this study, we observed that  $I_{DS}$  reduces slowly, which is approximately only 7% of the initial responsivity of the sensor (Fig.

3.11 (a)). Further, we have also performed electrical stability of the fabricated sensor for 50 consecutive cycles at RH 50% and temperature 25°C. We have seen only 6% change in the response with respect to the first cycle (Fig. 3.11 (b)).

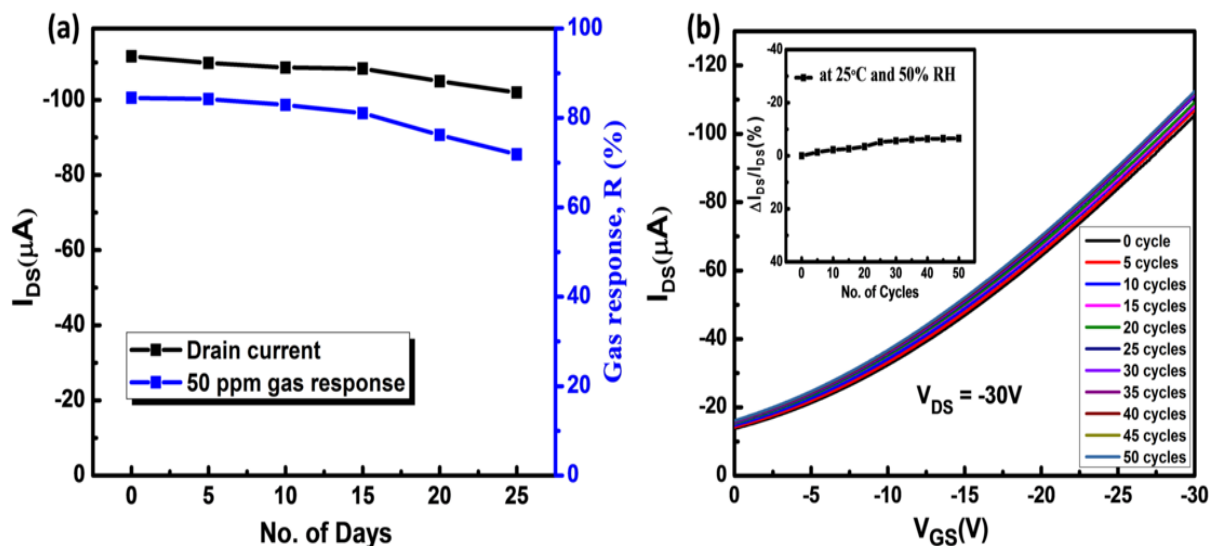


**Fig. 3.11.** (a) Environmental stability of the OTFT sensor and; (b) Electrical stability for 50 consecutive cycles at RH 50% and temperature 25°C.

The following findings demonstrate that the PBTTT-C14/MoS<sub>2</sub>-QDs based OTFT sensor has quite good stability, which can be an excellent choice for the detection of ammonia at around room temperature within a wide range of relative humidity.

A comparative performance of the PBTTT-C14/MoS<sub>2</sub>-QDs based OTFT sensor w.r.t the earlier reports are given in the Table-3.2.

Table-3.2: Comparative performance of the NH<sub>3</sub> sensor w.r.t the earlier reports.

Sensing material	Film deposition technique	Device configuration	Gas concentration	Response	Remark
PQT-12	Drop cast	MSM	100 PPM	Very low	Low sensitivity [129]
P3HT/Poly-styrene	Spin coat	Transistor	50 PPM	51%	Poor response [113]
Pentacene	Thermal evaporation	Transistor	100 PPM	14.8%	Poor response and recovery [130]
P3HT	Air-brush deposition	Transistor	100 PPM	19%	Low sensitivity [131]
PQT-12	FTM	Transistor	80 PPM	56.4%	Slower response [125]
PBTTT/MoS <sub>2</sub> -QDs (This work)	FTM	Transistor	50 PPM	Acc. Mode res.- 84.66% (50 ppm), dep. Mode (Off current factor)- $3 \times 10^3$	Cost-effective, Highly sensitive, Quick response

## 3.3.7. Sensing mechanism

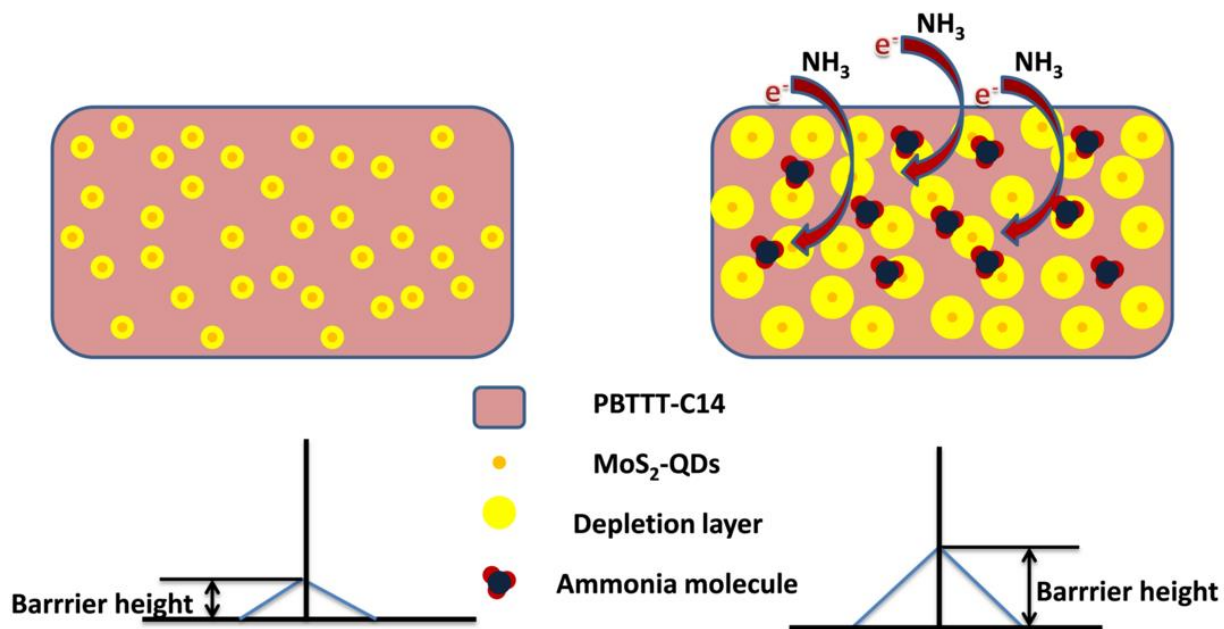


**Fig. 3.12** Ammonia sensing mechanism of the PBTTT-C14/MoS<sub>2</sub>-QDs hybrid based OTFT sensor.

The enhancement of the NH<sub>3</sub> sensing of the fabricated PBTTT-C14/MoS<sub>2</sub>-QDs hybrid film based OTFT sensor can be realized from the enhancement of depletion layer and the potential barrier height of PBTTT-C14/MoS<sub>2</sub>-QDs heterojunction. Since PBTTT-C14 and MoS<sub>2</sub>-QDs are p- and n-type semiconductor respectively [132, 133], therefore their heterojunction will form a depletion by transferring hole from PBTTT-C14 to MoS<sub>2</sub>-QDs and electron from MoS<sub>2</sub>-QDs to PBTTT-C14 until their Fermi level comes in the same level. This depletion layer will form a barrier height during charge transfer (hole) through this composite thin film. As NH<sub>3</sub> is a reductive (electron-donating) gas [134, 135], it will reduce the hole concentration of exposed area of the PBTTT-C14 film which will lead to the enhancement in depletion layer width in the exposed surface part of the film (Fig. 3.12). Therefore, net mobile charge carrier concentration of the PBTTT-C14 polymer will decrease and the overall sheet resistance of the PBTTT-

C14/MoS<sub>2</sub>-QDs channel will increase. Besides, barrier height of the mobile charges will also increase due the enhancement of the depletion layer width of the PBTTT-C14/MoS<sub>2</sub>-QDs heterojunction.

Moreover, this will lead to the change in various OTFT parameters including ON/OFF ratio, threshold voltage ( $V_{Th}$ ) of the device and effective carrier mobility ( $\mu$ ). It is known that the OFF current of an OTFT depends on two primary factors. One is the gate leakage current and the other one is the sheet resistance of the semiconductor channel. Assuming the gate leakage current of the OTFT will remain the same during gas sensitivity study, if sheet resistance of PBTTT-C14/MoS<sub>2</sub>-QDs hybrid film increases, the OFF current of the OTFT should be reduced. Fig. 3.13(c) shows that the OFF current of the device gradually decreases with concentration of NH<sub>3</sub> which supports the enhancement of the depletion layer of the PBTTT-C14/MoS<sub>2</sub>-QDs heterojunction. Fig. 3.13(d) shows the ‘off current factor’ (ratio of OFF current in absence to presence of NH<sub>3</sub> gas) of the devices. This data indicates that the variation of OFF current factor in case of hybrid device is  $\sim 3 \times 10^3$  when the NH<sub>3</sub> gas concentration changes from 0 to 50 ppm. This variation is several orders larger than the ON current variation of the device. Moreover, it has a good linearity  $>1$  ppm concentration of NH<sub>3</sub>. Though, the variation of this factor is almost negligible in case of Device-1 compared to the Device-2. Besides, due to this enhancement of the depletion layer, depleted charge accumulation in the dielectric/semiconductor increases, this leads to a shifting of  $V_{Th}$  of the OTFT device. Fig. 3.13(a) shows that the Device-2 has a shift of  $V_{Th}$  of  $\sim 19$  V when the concentration of NH<sub>3</sub> changes from 0 to 50 ppm. However, this shifting of  $V_{Th}$  in case of pristine PBTTT-C14 based OTFT is only  $\sim 1.5$  V, which simply indicates that enhancement of depletion layer of PBTTT-C14/MoS<sub>2</sub>-QDs heterojunction in presence of NH<sub>3</sub> is key reason for shifting of  $V_{Th}$  of the device. Besides, it has been observed from the Fig. 3.13(b)

the effective carrier mobility of the device also reduces from  $0.045$  to  $0.028$   $\text{cm}^2 \text{V}^{-1}\text{sec}^{-1}$  when the concentration of  $\text{NH}_3$  changes from 0 to 50 ppm. Although,  $\mu$  varies from  $0.03$  to  $0.024$   $\text{cm}^2 \text{V}^{-1}\text{sec}^{-1}$  in case of Device-1 (Fig. 3.7b). The larger reduction of  $\mu$  in case of polymer/QDs hybrid film is due to the enhancement of barrier height of the accumulated hole carrier of the channel.

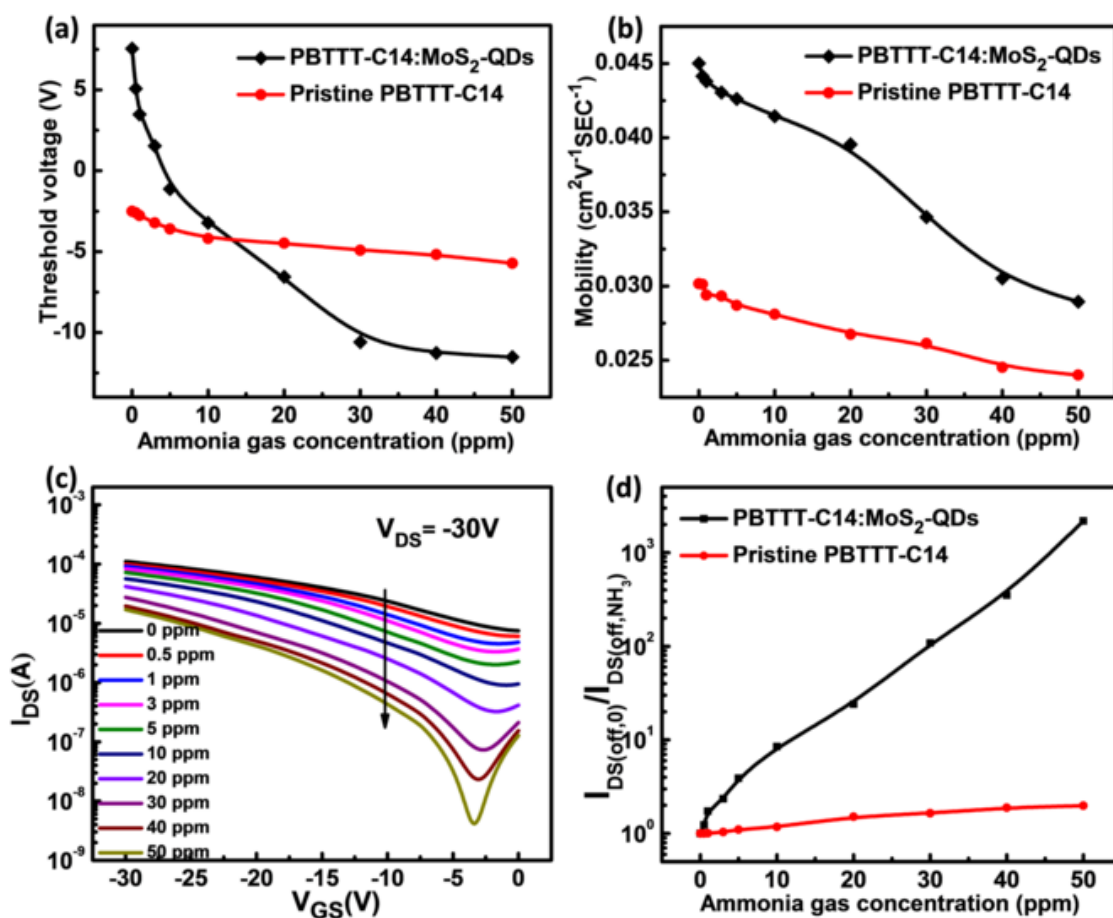


**Fig. 3.13.** Schematic representation of variation in (a) Threshold voltage, (b) mobility; (c) off current variation in PBTTT-C14/MoS<sub>2</sub>-QDs heterojunction based OTFT, and (d) off current factor with the ammonia concentration ranging from 0 to 50 ppm.

**3.4. Conclusion**

A highly sensitive OTFT-based NH<sub>3</sub> sensor has been fabricated by using PBTTT-C14/MoS<sub>2</sub>-QDs heterojunction thin film. Colloidal QDs of MoS<sub>2</sub> have been synthesized by a hydrothermal method, whereas heterojunction thin film has been deposited by a simple, low-cost and high yield 'floating film transfer method'. A reference OTFT of pristine PBTTT-C14 has been fabricated under the same condition. Our comparative study reveals that the depletion layer of PBTTT-C14/MoS<sub>2</sub>-QDs heterojunction is extremely sensitive to the NH<sub>3</sub> gas which has been working as a hot-spot for this gas sensor. Due to a very small variation of gas concentration, a large variation of device parameters has been observed which enables us to reach a response of 85% at 50 ppm concentration of NH<sub>3</sub> that has been calculated from the ON current variation of the device. This value is ~3 times higher w.r.t the reference OTFT. However, the OFF current variation of this OTFT is much more sensitive and shows a variation of  $\sim 3 \times 10^3$  times in presence of 50 ppm NH<sub>3</sub> which also becomes possible due to the large variation of the depletion layer of the heterojunction. Besides, this OTFT shows a very high selectivity with good linearity to the gas concentration. Moreover, this OTFT is capable of measuring low concentration of NH<sub>3</sub> up to the level of 500 ppb. Overall this polymer/QDs heterojunction based OTFT sensor that has been fabricated in a very easy and low-cost method is capable of fulfilling all basic features for its practical application as NH<sub>3</sub> sensor.